PHYSICAL REVIEW A **98**, 022504 (2018)

Dynamic electron-correlation energy in the natural-orbital-functional second-order-Møller-Plesset method from the orbital-invariant perturbation theory

Mario Piris
Kimika Fakultatea, Euskal Herriko Unibertsitatea (UPV/EHU), P.K. 1072, 20080 Donostia, Euskadi, Spain;
Donostia International Physics Center (DIPC), 20018 Donostia, Euskadi, Spain;
and IKERBASQUE, Basque Foundation for Science, 48013 Bilbao, Euskadi, Spain

(Received 26 May 2018; revised manuscript received 5 July 2018; published 10 August 2018)

The original formulation [M. Piris, Phys. Rev. Lett. **119**, 063002 (2017)] of the natural-orbital-functional second-order-Møller-Plesset (NOF-MP2) method is based on the MP2 that uses the canonical Hartree-Fock molecular orbitals. The current work presents a reformulation of the dynamic energy correction based on the orbital-invariant MP2, which allows one to attain both dynamic and static correlations even for those systems with strong orbital localizability and significant multiconfigurational character. To improve the reference Slater determinant formed with natural orbitals, the natural orbital functional that generates them is also modified to take into account only the interpair static correction. This more general NOF-MP2 is able to dissociate properly noble-gas dimers, which remain as nonbound species within the canonical formulation. Test calculations in a selected set of 30 polyatomic molecules demonstrate a substantial improvement not only of the relative energies, but also of the total energies calculated with the NOF-MP2 method.

DOI: 10.1103/PhysRevA.98.022504

A reliable electronic structure method must be able to describe, in a balanced way, both static (nondynamic) and dynamic electron correlation [1,2]. Recently [3], a single-reference global method for electron correlation was introduced, taking as reference the Slater determinant of natural orbitals (NOs) obtained from an approximate natural orbital functional (NOF) [4]. In this approach, the total energy is formed as $\tilde{E}_{hf} + E^{\rm dyn} + E^{\rm sta}$, where $\tilde{E}_{hf}$ is the Hartree-Fock (HF) energy obtained with NOs, the dynamic energy ($E^{\rm dyn}$) is derived from a modified second-order-Møller-Plesset perturbation theory (MP2), while the nondynamic energy ($E^{\rm sta}$) is obtained from the static component of the NOF.

The success of the method, called NOF-MP2, is determined by the NOs used to generate the reference. In [3], orbitals were obtained from the Piris natural-orbital-functional 7 (PNOF7) there proposed: an interacting-pair model that recovers the intrapair but only static interpair correlation. As a consequence, PNOF7 NOs can be localized in certain regions of space, depending on the degree of interaction between the electron pairs. When the interpair nondynamic correlation is negligible, these orbitals turn out to be close to the known NOs of the independent-pair model (PNOF5) [5]. In general, NOs will be located in those regions where their atomic orbitals responsible for the intrapair and static correlation are found. It is worth noting that localized NOs provide an orbital picture with a clear chemical meaning [6] that is not easy to obtain using canonical orbitals.

On the other hand, $E^{\rm dyn}$ was formulated [3] from traditional MP2 energy that involves the use of canonical HF molecular orbitals; therefore, a reformulation of dynamic energy correction is necessary so that any type of orbital can be used. Perturbation theory with noncanonical orbitals (in most cases, localized orbitals) has been formerly used [7,8] in order to speed up processing times. As Pulay pointed out [9], the increase in computational cost associated with the increase in the number of electrons is not justified and is mainly due to the use of canonical orbitals. In the last three decades, the orbital localizability has been exploited by several approaches known as linear-scaling methods [10]. The latter have extended the applicability of wave-function-based correlation methods to larger electronic systems. Consequently, an additional motivation for a reformulation of $E^{\rm dyn}$ is the possibility of computer savings.

The present work pursues two objectives: on the one hand, improve NOs with which the reference determinant is built and, on the other hand, propose a correction $E^{\rm dyn}$ based on the orbital-invariant (OI) MP2 energy. As a result, a variant of the method we will call NOF-OIMP2 emerges, whereas from now on we will refer to the original version as NOF-canonical MP2 (NOF-cMP2).

In NOF theory [11,12], the ground-state electronic energy (E) is given in terms of the NOs $\{\phi_i\}$ and their occupation numbers (ONs) $\{n_i\}$. Unfortunately, the exact reconstruction $E[\{n_i,\phi_i\}]$ has been an unattainable goal so far; therefore we are talking about orbitals that diagonalize the one-particle reduced density matrix (1-RDM) corresponding to an approximate ground-state energy, and it is more appropriate to talk about NOF instead of a 1-RDM functional due to the existing dependence on the reconstructed two-particle RDM (2-RDM).

Restrictions on the ONs in the range $0 \leqslant n_i \leqslant 1$ represent the necessary and sufficient conditions for ensemble N-representability of 1-RDM [13] under the normalization condition $\sum_i n_i = N$. Note that we focus on the N-representability problem for statistical one-matrix ensembles since to guarantee the pure-state N-representability conditions [14,15], only 1-RDM ensemble constraints are necessary if $E[\{n_i,\phi_i\}]$ is a pure N-representable functional [16,17].

2469-9926/2018/98(2)/022504(6)

In approximate one-particle theories, the 2-RDM plays a dominant role that determines the functional *N*-representability [4]. The use of 2-RDM ensemble *N*-representability conditions [18] for generating a reconstruction functional was proposed in Ref. [19], where auxiliary matrices Δ and Π were introduced to reconstruct the two-particle cumulant [20]. In this paper, we address only singlet states and adopt a restricted spin theory, so that energy reads

$$E = 2\sum_{p} n_p \mathcal{H}_{pp} + \sum_{qp} \Pi_{qp}\mathcal{L}_{pq} + \sum_{qp}(n_q n_p - \Delta_{qp})(2\mathcal{J}_{pq} - \mathcal{K}_{pq}), \quad (1)$$

where $\mathcal{H}_{pp}$ denotes the diagonal elements of the core Hamiltonian, while $\mathcal{J}_{pq}$, $\mathcal{K}_{pq}$, and $\mathcal{L}_{pq}$ are the direct, exchange, and exchange-time-inversion [21] integrals. Appropriate forms of matrices Δ and Π lead to different implementations known in the literature as PNOF*i* ($i = 1$–7) [3,22,23]. The case of PNOF5 [24,25] is remarkable, which turned out to be pure *N*-representable [26,27].

The conservation of the total spin allows one to derive the diagonal elements $\Delta_{pp} = n_p^2$ and $\Pi_{pp} = n_p$ [28]. The 2-RDM *N*-representability *D* and *Q* conditions lead to inequalities $\Delta_{qp} \leqslant n_q n_p$ and $\Delta_{qp} \leqslant h_q h_p$ [19], where $h_p = 1 - n_p$. To fulfill the *G* condition, the off-diagonal elements of the Π matrix must satisfy the constraint [29]

$$\Pi_{qp}^2 \leqslant (n_q h_p + \Delta_{qp})(h_q n_p + \Delta_{qp}). \quad (2)$$

For a given approximation of Δ_{qp}, it is evident that the modulus of Π_{qp} is determined from Eq. (2) assuming the equality; however, there is no hint to determine the sign of Π_{qp}. The requirement that for any two-electron singlet the NOF (1) yields the accurate energy expression obtained from the exact wave function [30] implies [29] that $\Delta_{qp} = n_q n_p$ and $|\Pi_{qp}| = \sqrt{n_q n_p}$, respectively. Furthermore, the phase factor of Π_{qp} can be $+1$ if $q, p \in (1, \infty)$, and -1 otherwise.

To achieve a model of independent pairs with $N > 2$, the orbital space Ω is divided into $N/2$ mutually disjoint subspaces Ω_g, so each subspace contains one orbital g below the level $N/2$, and N_g orbitals above it, which is reflected in additional sum rules for the ONs ($\sum n_p = 1$, $p \in \Omega_g$). In what follows, let us consider N_g equal to a fixed number that corresponds to the maximum value allowed by the basis set that is used. Keeping $\Delta_{qp} = n_q n_p$ and generalizing the two-electron expression for off-diagonal elements of the Π matrix, namely, $\Pi_{qp}^g = \sqrt{n_q n_p}$ if $q, p > N/2$, and $\Pi_{qp}^g = -\sqrt{n_q n_p}$ if $q = g$ or $p = g$, we obtain the extended PNOF5 [25].

In Ref. [3], nonzero Π_{qp} elements were considered among orbitals belonging to different subspaces [3], whereas $\Delta_{qp} = 0$. From Eq. (2) follows that provided the Δ_{qp} vanishes, $|\Pi_{qp}| \leqslant \Phi_q \Phi_p$ with $\Phi_q = \sqrt{n_q h_q}$. Assuming equality, and generalization of the sign convention adopted for extended PNOF5, i.e., $\Pi_{qp}^\Phi = \Phi_q \Phi_p$ if $q, p > N/2$, and $\Pi_{qp}^\Phi = -\Phi_q \Phi_p$ otherwise, led to PNOF7 [3].

Another possible option, which favors decreasing of the energy (1), is to consider all the interpair factors to be negative, ergo, $\Pi_{qp}^\Phi = -\Phi_q \Phi_p$. Recently [31], we have analyzed several examples with strong static correlation, specifically the one-dimensional Hubbard model with up to 14 sites and rings with up to 16 hydrogens. Compared with accurate diagonalization calculations, our results indicate that all-negative interpair factors is a better option.

In addition, it would be convenient to take into account the interpair static correction in the NOF from the outset, thus preventing the ONs and NOs from suffering an interpair nondynamic influence, however small, in the dynamic correlation domains. Taking into account the fg-th interpair static correlation energy [3],

$$E_{fg}^{\rm sta} = \sum_{p\in\Omega_f}\sum_{q\in\Omega_g} 4\Phi_p\Phi_q\,\Pi_{qp}^{\Phi}\,\mathcal{L}_{pq} = \sum_{p\in\Omega_f}\sum_{q\in\Omega_g} \Pi_{qp}^{s}\,\mathcal{L}_{pq}, \quad (3)$$

we attain the following NOF:

$$E = \sum_{g=1}^{N/2}\sum_{p\in\Omega_g}\left[n_p(2\mathcal{H}_{pp} + \mathcal{J}_{pp}) + \sum_{q\in\Omega_g, q\neq p}\Pi_{qp}^g\mathcal{L}_{pq}\right] + \sum_{f\neq g}^{N/2}\sum_{p\in\Omega_f}\sum_{q\in\Omega_g}\left[n_q n_p(2\mathcal{J}_{pq} - \mathcal{K}_{pq}) + \Pi_{qp}^s\mathcal{L}_{pq}\right], \quad (4)$$

where $\Pi_{qp}^s = -4 n_q h_q n_p h_p$. This approach will henceforth be referred to as PNOF7s and will provide the reference NOs to form $\tilde{E}_{hf}$ in the NOF-OIMP2 method. The "s" in PNOF7s emphasizes that this interacting-pair model takes into account only the static correlation between pairs, and therefore avoids double counting in the regions where the dynamic correlation predominates, already in the NOF optimization.

Like PNOF7, PNOF7s produces qualitatively correct potential-energy curves (PECs) for the dozen diatomic molecules studied in Ref. [3]. These systems cover a wide range of values for binding energies (D_e) and bond lengths (R_e); however, in all cases, the correct dissociation limit implies a homolytic cleavage of the bond with a high degree of degeneracy effects. In Table I, a comparison between both functionals is shown. The experimental bond lengths are

TABLE I. Comparison between PNOF7 and PNOF7s using the cc-pVTZ basis set.

	R_e (Å)			D_e (kcal/mol)		
Molecule	PNOF7	PNOF7s	Expt.	PNOF7	PNOF7s	Expt.
H_2	0.743	0.743	0.743	108.6	108.6	109.5
LiH	1.604	1.603	1.595	56.1	56.4	58.0
Li_2	2.667	2.644	2.673	23.3	23.4	24.4
BH	1.232	1.228	1.232	75.7	81.0	81.5
OH^-[a]	0.966	0.961	0.964	87.0	93.6	
HF	0.915	0.918	0.917	106.7	114.4	141.1
LiF	1.576	1.561	1.564	95.4	104.6	139.0
N_2	1.097	1.089	1.098	188.9	181.2	228.3
CN^-[a]	1.186	1.169	1.177	212.0	202.7	240.7
CO	1.120	1.115	1.128	178.1	191.4	259.3
NO^+	1.056	1.048	1.063	179.9	189.8	
F_2	1.579	1.502	1.412	2.6	10.1	39.2

[a] aug-cc-pVTZ was used.

taken from the National Institute of Standards and Technology (NIST) Database [32], whereas the experimental dissociation energies result from a combination of Refs. [32] and [33]. The correlation-consistent valence triple-ζ basis set (cc-pVTZ) developed by Dunning [34] was used throughout, except for the anionic species where the augmented basis set (aug-cc-pVTZ) was used.

Table I shows a slight shortening of the equilibrium distances obtained with PNOF7s compared to those obtained with PNOF7, whereas the dissociation energies experience a slight increase, except in the cases of N_2 and CN^-. These minor effects are related to the prevention of considering nondynamic correlation between pairs in the equilibrium regions where the dynamic correlation prevails, and should lead to an improvement in the R_e and D_e calculated with the NOF-MP2 method. As was pointed out in [3], the results are in good agreement with the experiment for the smaller diatomics, for which the electron-correlation effect is almost entirely intrapair. When the number of pairs increases, the theoretical values deteriorate, especially for the dissociation energies. This is related to a better description of the asymptotic region with respect to the equilibrium, and therefore it is necessary to add the dynamic electron correlation between pairs.

Now we focus on the reformulation of E^{dyn}. In the 1980s, Pulay and Saebø introduced an orbital-invariant formulation of MP2, the details of which can be found elsewhere [7,35]. The first-order wave function is a linear combination of all doubly excited configurations, and their amplitudes T_{pq}^{fg} are obtained by solving the equations for the MP2 residuals. The MP2 energy correction takes the form

$$E^{(2)} = \sum_{g,f=1}^{N/2} \sum_{p,q>N/2}^{M} \langle gf|pq\rangle \left[2T_{pq}^{gf} - T_{pq}^{fg}\right], \tag{5}$$

where M is the number of basis functions and $\langle gf|pq\rangle$ are the matrix elements of the two-particle interaction.

In NOF-cMP2, E^{dyn} is obtained as the canonical $E^{(2)}$ modified to avoid double counting of the electron correlation [3]. The latter is divided into intra- and interpair contributions, and the amount of dynamic correlation in each orbital p is defined by functions C_p of its occupancy, namely,

$$C_p^{\text{intra}} = \begin{cases} 1 - 4h_p^2, & p \leqslant N/2 \\ 1 - 4n_p^2, & p > N/2, \end{cases}$$
$$C_p^{\text{inter}} = \begin{cases} 1, & p \leqslant N/2 \\ 1 - 4h_p n_p, & p > N/2. \end{cases} \tag{6}$$

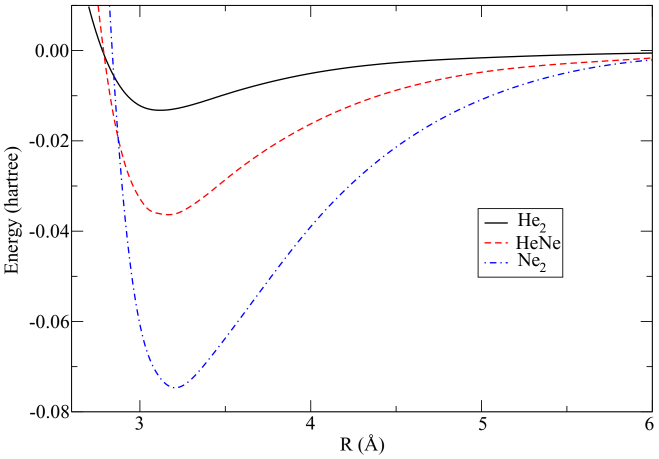

FIG. 1. Potential-energy curves of noble-gas dimers calculated at the NOF-OIMP2/aug-cc-pVTZ level of theory. The zero-energy point has been set at 10 Å for each system.

According to Eq. (6), fully occupied and empty orbitals yield a maximal contribution to dynamic correlation, whereas orbitals with half occupancies contribute nothing. It is worth noting that C_p^{inter} is not considered if the orbital is below $N/2$. Using these functions as the case may be (intrapair or interpair), we define modified off-diagonal elements of the Fock matrix ($\tilde{\mathcal{F}}$) as

$$\tilde{\mathcal{F}}_{pq} = \begin{cases} C_p^{\text{intra}} C_q^{\text{intra}} \mathcal{F}_{pq}, & p,q \in \Omega_g \\ C_p^{\text{inter}} C_q^{\text{inter}} \mathcal{F}_{pq}, & \text{otherwise}, \end{cases} \tag{7}$$

as well as modified two-electron integrals,

$$\widetilde{\langle pq|rt\rangle} = \begin{cases} C_p^{\text{intra}} C_q^{\text{intra}} C_r^{\text{intra}} C_t^{\text{intra}} \langle pq|rt\rangle, & p,q,r,t \in \Omega_g \\ C_p^{\text{inter}} C_q^{\text{inter}} C_r^{\text{inter}} C_t^{\text{inter}} \langle pq|rt\rangle, & \text{otherwise}, \end{cases} \tag{8}$$

where the subspace index $g = 1, \ldots, N/2$. This leads to the following linear equation for the modified MP2 residuals:

$$\begin{aligned} \tilde{R}_{ab}^{ij} &= \widetilde{\langle ab|ij\rangle} + (\mathcal{F}_{aa} + \mathcal{F}_{bb} - \mathcal{F}_{ii} - \mathcal{F}_{jj}) T_{ab}^{ij} \\ &\quad + \sum_{c\neq a} \tilde{\mathcal{F}}_{ac} T_{cb}^{ij} + \sum_{c\neq b} T_{ac}^{ij} \tilde{\mathcal{F}}_{cb} - \sum_{k\neq i} \tilde{\mathcal{F}}_{ik} T_{ab}^{kj} \\ &\quad - \sum_{k\neq j} T_{ab}^{ik} \tilde{\mathcal{F}}_{kj} = 0, \end{aligned} \tag{9}$$

where i, j, k refer to the strong occupied NOs, and a, b, c to weak occupied ones. It should be noted that diagonal elements of the Fock matrix ($\mathcal{F}$) are not modified.

By solving the linear system of Eqs. (9), the amplitudes T_{pq}^{fg} are obtained, which are inserted into Eq. (5) to achieve $E^{\text{dyn}} = E^{(2)}$. Following Ref. [3], the total energy of the system will be given by

$$E = \tilde{E}_{hf} + E^{\text{corr}} = \tilde{E}_{hf} + E^{\text{sta}} + E^{\text{dyn}}, \tag{10}$$

TABLE II. Comparison of R_e(Å) and D_e(kcal/mol) calculated at the MP2 and NOF-OIMP2 levels of theory with the experimental values. The aug-cc-pVTZ basis set was used.

	MP2		NOF-OIMP2		Experiment	
Dimer	R_e	D_e	R_e	D_e	R_e	D_e
He$_2$	3.09	0.013	3.12	0.013	2.97	0.022
HeNe	3.12	0.038	3.17	0.035	3.03	0.041
Ne$_2$	3.18	0.076	3.21	0.074	3.09	0.084

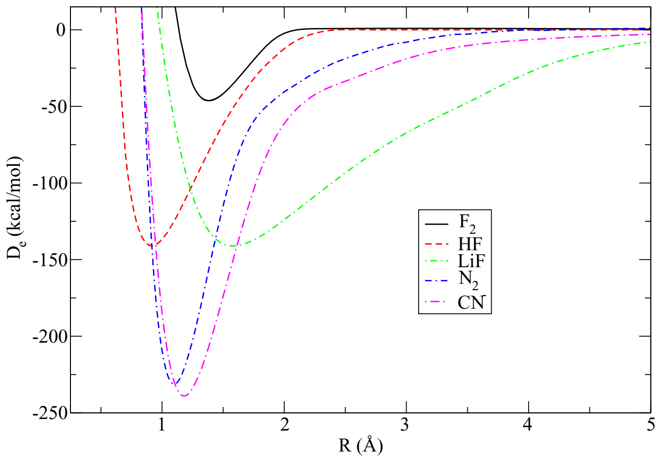

FIG. 2. Potential-energy curves with homolytic cleavage of the bond calculated at the NOF-OIMP2/cc-pVTZ level of theory. The zero-energy point has been set at 10 Å for each system.

where $\tilde{E}_{hf}$ is the HF energy obtained with the NOs of PNOF7s, given by Eq. (4), and $E^{\rm sta}$ is the sum of energies (3),

$$E^{\rm sta}_{\rm inter} = \sum_{f\neq g}^{N/2} E^{\rm sta}_{fg} = \sum_{f\neq g}^{N/2}\sum_{p\in\Omega_f}\sum_{q\in\Omega_g}\Pi^{s}_{qp}\,\mathcal{L}_{pq}, \qquad (11)$$

plus the static intrapair electron correlation energy [3],

$$E^{\rm sta}_{\rm intra} = \sum_{g=1}^{N/2}\sum_{q\neq p}\sqrt{\Lambda_q\Lambda_p}\,\Pi^{g}_{qp}\,\mathcal{L}_{pq}. \qquad (12)$$

In Eq. (12), note that $q,\ p\in\Omega_g$, and $\Lambda_p = 1-|1-2n_p|$ is the amount of intrapair static electron correlation in each orbital p as a function of its occupancy.

The performance of NOF-OIMP2 has been tested in several examples. Let us start with noble-gas dimers, which are held together by dispersion, a manifestation of long-range dynamic correlation. These species are not bound at the PNOF7 level of theory, and they remain so even after adding $E^{\rm dyn}$ using the canonical formulation. With the formulation of $E^{\rm dyn}$ based on the orbital-invariant MP2, the orbital localizability in noble-gas atoms can now be taken into account, so that NOF-OIMP2 predicts bound species.

The potential-energy curves (PECs) of He_2, HeNe, and Ne_2 are depicted in Fig. 1. For each of the curves, the zero-energy point has been set at their corresponding energy at 10 Å. It can be seen that NOF-OIMP2 produces qualitatively correct PECs. In Table II, the equilibrium bond lengths (R_e) and dissociation energies (D_e) at the MP2 and NOF-OIMP2 levels of theory can be found. The experimental values were taken from Ref. [36]. The augmented correlation-consistent valence triple-ζ basis set (aug-cc-pVTZ) [37,38] was used in theoretical calculations. It is worth noting that a larger basis set is needed to adequately compare them with the experiment. In addition, only valence electrons have been included in the correlation treatment. It can be observed that both methods underestimate the binding energies and overestimate the equilibrium distances since these effects are more perceptible for the NOF-OIMP2. He2 is the worst case since only 60% of the binding energy is recovered, while for the other two systems it is between 85 and 92%.

There are no significant differences between the results obtained with the NOF-cMP2 and NOF-OIMP2 methods for diatomic systems analyzed in Table I. Representative PECs of these molecules are depicted in Fig. 2. Table III collects the electronic properties previously analyzed for systems shown in Fig. 2. The data reveal an outstanding improvement in the dissociation energies with respect to PNOF7 and PNOF7s, respectively. A slight improvement of the theoretical equilibrium distances calculated with NOF-OIMP2 is also observed over those obtained with NOF-cMP2.

The situation is quite different in polyatomic systems where the orbital localizability drastically changes the results obtained with NOF-cMP2 and NOF-OIMP2. Both methods have been tested on a set of 30 selected molecules with a dominant dynamic electron correlation to compare with reliable MP2 energies. We must be aware that the applicability of standard MP2 is restricted to cases without static correlation; otherwise, we obtain an excess of correlation energy. An example is the case of ozone which has an important multiconfigurational character. In this case, NOF-OIMP2 predicts a total energy that is about 57 kcal/mol higher than the MP2 value for the cc-pVTZ basis set [34]. Consequently, an upper bound to the total MP2 energy can be expected in most cases since a fraction, however small, of nondynamic correlation is present.

The collection of total energies for the selected set of molecules, calculated at their experimental geometries [39] using the cc-pVTZ basis set [34], can be found in Table IV. For the whole set, the average differences in the NOF-cMP2 and NOF-OIMP2 energies from MP2 are 34.5 and 6.3 mHartree, respectively. The data reveal an outstanding improvement in the total energies of the NOF-OIMP2 over the NOF-cMP2.

To summarize, it has been shown that a reformulation of the dynamic electron-correlation energy based on the orbital-invariant MP2 allows one to extend the NOF-MP2 method to

TABLE III. Comparison between NOF-cMP2 and NOF-OIMP2 using the cc-pVTZ basis set.

	R_e (Å)			D_e (kcal/mol)		
Molecule	NOF-cMP2	NOF-OIMP2	Expt.	NOF-cMP2	NOF-OIMP2	Expt.
F_2	1.397	1.382	1.412	34.5	46.0	39.2
HF	0.924	0.916	0.917	139.4	140.9	141.1
LiF	1.614	1.579	1.564	140.7	141.1	139.0
N_2	1.084	1.098	1.098	224.2	230.7	228.3
CN^{-} [a]	1.180	1.180	1.177	238.6	239.0	240.7

[a] aug-cc-pVTZ was used.

TABLE IV. Comparison of total electronic energies, in Hartrees, calculated using the cc-pVTZ basis set at the experimental geometry.

No.	Molecule	NOF-cMP2	NOF-OIMP2	MP2
1	H_2O	−76.316438	−76.317906	−76.320480
2	NH_3	−56.447022	−56.452165	−56.454549
3	CH_4	−40.404095	−40.411188	−40.412721
4	HCN	−93.212795	−93.216612	−93.223664
5	C_2H_2	−77.148255	−77.154876	−77.160778
6	PH_3	−342.643167	−342.657773	−342.661029
7	Si_2H_6	−581.624090	−581.641714	−581.643376
8	H_2CO	−114.288902	−114.301503	−114.309339
9	H_2S	−398.885411	−398.903604	−398.907289
10	C_2H_4	−78.378826	−78.397165	−78.401267
11	CH_3OH	−115.494590	−115.514704	−115.519139
12	H_2O_2	−151.308915	−151.325929	−151.334177
13	BF_3	−324.146891	−324.165476	−324.172517
14	C_2H_6	−79.603872	−79.628190	−79.631938
15	CH_3NH_2	−95.631675	−95.655525	−95.659988
16	N_2H_4	−111.629997	−111.655618	−111.661187
17	HOCl	−535.330974	−535.356795	−535.363297
18	C_3H_4	−116.358023	−116.383694	−116.392120
19	CH_3Cl	−499.486888	−499.518970	−499.522907
20	CH_3SH	−438.083227	−438.117335	−438.123037
21	C_2FH_3	−177.487929	−177.523874	−177.532492
22	CH_3OCH_3	−154.679334	−154.720399	−154.727219
23	C_3H_6	−117.568157	−117.614170	−117.620957
24	C_2H_4O	−153.450942	−153.496429	−153.504674
25	HCF_3	−337.770010	−337.814755	−337.824683
26	C_2H_5N	−133.585955	−133.635764	−133.643763
27	COF_2	−312.560599	−312.607818	−312.620274
28	CO_2	−188.249006	−188.301643	−188.311990
29	OCS	−510.822787	−510.878940	−510.891218
30	BCl_3	−1403.962819	−1404.036515	−1404.045130

any type of orbitals, including the typical localized orbitals of electron-pair-based NOFs. The global character of the method was demonstrated in terms of relative and total energies since the dynamic and static correlation can be recovered in one shot for any type of system, including weakly bound van der Waals species.

The author thanks Fred Manby for his useful suggestions during the ESCMQC2017. The SGI/IZO-SGIker of UPV/EHU supported by European funding (ERDF and ESF) is gratefully acknowledged for generous allocation of computational resources. The support from MINECO (Grant No. CTQ2015-67608-P) is also acknowledged.

---

[1] E. Valderrama, E. V. Ludeña, and J. Hinze, J. Chem. Phys. **106**, 9227 (1997).

[2] E. Valderrama, E. V. Ludeña, and J. Hinze, J. Chem. Phys. **110**, 2343 (1999).

[3] M. Piris, Phys. Rev. Lett. **119**, 063002 (2017).

[4] M. Piris, in *Many-body Approaches at Different Scales: A Tribute to N. H. March on the Occasion of his 90th Birthday*, edited by G. G. N. Angilella and C. Amovilli (Springer, New York, 2018), Chap. 22, pp. 283–300.

[5] M. Piris, J. M. Matxain, X. Lopez, and J. M. Ugalde, Theor. Chem. Acc. **132**, 1298 (2013).

[6] J. M. Matxain, M. Piris, J. Uranga, X. Lopez, G. Merino, and J. M. Ugalde, Chem. Phys. Chem. **13**, 2297 (2012).

[7] S. Saebo, in *Computational Chemistry: Reviews of Current Trends*, edited by J. Leszczynski (World Scientific, Singapore, 2002), Vol. 7, pp. 63–87.

[8] H. J. Werner, G. Knizia, C. Krause, M. Schwilk, and M. Dornbach, J. Chem. Theor. Comput. **11**, 484 (2015).

[9] P. Pulay, Chem. Phys. Lett. **100**, 151 (1983).

[10] *Linear-Scaling Techniques in Computational Chemistry and Physics*, edited by R. Zalesny, M. G. Papadopoulos, P. G. Mezey, and J. Leszczynski (Springer, New York, 2011).

[11] M. Piris, in *Reduced-Density-Matrix Mechanics: With Applications to Many-Electron Atoms and Molecules*, edited by D. A. Mazziotti (John Wiley and Sons, Hoboken, NJ, 2007), Chap. 14, pp. 387–427.

[12] M. Piris and J. M. Ugalde, Int. J. Quantum Chem. **114**, 1169 (2014).

[13] A. J. Coleman, Rev. Mod. Phys. **35**, 668 (1963).

[14] A. A. Klyachko, J. Phys.: Conf. Ser. **36**, 72 (2006).

[15] M. Altunbulak and A. A. Klyachko, Commun. Math. Phys. **282**, 287 (2008).

[16] S. M. Valone, J. Chem. Phys. **73**, 1344 (1980).

[17] T. T. Nguyen-Dang, E. V. Ludeña, and Y. Tal, J. Mol. Struc.: THEOCHEM **120**, 247 (1985).

[18] D. A. Mazziotti, Phys. Rev. Lett. **108**, 263002 (2012).

[19] M. Piris, Int. J. Quantum Chem. **106**, 1093 (2006).

[20] D. A. Mazziotti, Chem. Phys. Lett. **289**, 419 (1998).

[21] M. Piris, J. Math. Chem. **25**, 47 (1999).

[22] M. Piris, Int. J. Quantum Chem. **113**, 620 (2013).

[23] M. Piris, J. Chem. Phys. **141**, 044107 (2014).

[24] M. Piris, X. Lopez, F. Ruipérez, J. M. Matxain, and J. M. Ugalde, J. Chem. Phys. **134**, 164102 (2011).

[25] M. Piris, J. M. Matxain, and X. Lopez, J. Chem. Phys. **139**, 234109 (2013).

[26] K. Pernal, Comp. Theor. Chem. **1003**, 127 (2013).

[27] M. Piris, J. Chem. Phys. **139**, 064111 (2013).

[28] M. Piris, J. M. Matxain, X. Lopez, and J. M. Ugalde, J. Chem. Phys. **131**, 021102 (2009).

[29] M. Piris, J. M. Matxain, X. Lopez, and J. M. Ugalde, J. Chem. Phys. **133**, 111101 (2010).

[30] P. O. Lowdin and H. Shull, Phys. Rev. **101**, 1730 (1955).

[31] I. Mitxelena, M. Rodríguez-Mayorga, and M. Piris, Eur. Phys. J. B **91**, 109 (2018).

[32] *NIST Standard Reference Database Number 101, Release 18*, edited by R. D. Johnson III (National Institute of Standards and Technology, Washington, DC, 2016).

[33] M. W. Chase, Jr., J. Phys. Chem. Ref. Data Monogr. **9**, 1 (1998).

[34] T. H. Dunning Jr., J. Chem. Phys. **90**, 1007 (1989).

[35] P. Pulay and S. Saebo, Theor. Chim. Acta **69**, 357 (1986).

[36] J. Ogilvie and F. Y. Wang, J. Mol. Struct. **273**, 277 (1992).

[37] R. A. Kendall, T. H. Dunning, Jr., and R. J. Harrison, J. Chem. Phys. **96**, 6796 (1992).

[38] D. E. Woon and T. H. Dunning, Jr., J. Chem. Phys. **100**, 2975 (1994).

[39] *NIST Computational Chemistry Comparison and Benchmark Database, NIST Standard Reference Database No. 101, Release 18*, edited by R. D. Johnson III (National Institute of Standards and Technology, Washington, DC, 2016), http://cccbdb.nist.gov/.